Cell Compatibility of Antimicrobial Electrospun Scaffolds

by

Andrew Talor Wong

Supervisor:
Prof. J. Paul Santerre
Meghan Wright

April 2015

Abstract

Periodontal disease, if left untreated, can eventually lead to tooth loss due to chronic inflammation in the periodontal space. During this process, gingival recession occurs, exposing the root of the tooth. Synthetic scaffolds may be used to create tissue engineered constructs to aid in the regeneration of the gingival tissues. An electrospun scaffold with an embedded antimicrobial polymer has been proposed for this purpose, and this study aims to characterize its cell compatibility properties. Cytocompatibility of the 7 day scaffold biodegradation and antimicrobial release products was tested with human gingival fibroblasts (HGFs) using a cell metabolic assay and DNA quantification. Results indicate that there is a reduction in the cell metabolic activity for cells exposed to the most concentrated solution of biodegradation and release products. Further investigation showed that the product responsible for the lowered metabolic activity is soluble and may be accumulating during the biodegradation study, as the cytotoxic effect was more pronounced for products taken from later time points of the study. However, the *in vivo* concentration of the release products is expected to be much lower due to constant circulation of fluids through the highly vascularized tissue. Results also indicate that the HGF cells are able to attach on the scaffolds and remain viable after 24 hours of culture. Overall, this study provides further insight on the cell compatibility of these scaffolds for their use as infection resistant tissue engineering scaffolds.

Acknowledgments

I would like to thank my supervisor, Professor J. Paul Santerre, for his guidance throughout this 4th year thesis. I really appreciate his personalized supervision and attention to this project, and am extremely grateful for this opportunity. I would also like to especially thank my graduate student supervisor, Meghan Wright, for being an excellent mentor throughout this entire thesis. Her dedication, knowledge, support, and encouragement resulted in the completion of this thesis and would not have been possible without her help. A special thanks to Dr. Jian Wang for his help with the SEM. As for the rest of the members of the Santerre lab, thank you for being such a supportive group of people and making me feel like a part of the family. This thesis was supported by NSERC Grant #360520.

Contents

List of Figures

List of Symbols

Symbol	Definition
BD	Butane diol
CF (AP)	Scaffold with drug in polymeric form
CF HCl	Scaffold with drug in free form
DMEM	Dulbecco's modified Eagle's medium
DMSO	Dimethyl sulfoxide
ECM	Extracellular matrix
EthD-1	Ethidium Homodimer-1 dead cell stain
FBS	Fetal bovine serum
GM	Growth medium
HDI	Hexane diisocyanate
HFIP	Hexafluoroisopropanol
HGF	Human gingival fibroblast
MMP	Matrix metalloproteinases
PBS	Phosphate buffered saline
PBS(+/+)	PBS with $MgCl_2$ and $CaCl_2$
PCN	Polyhexamethylene carbonate diol
PU	Polyurethane
SE	Standard error
SEM	Scanning electron microscope

Chapter 1

Introduction

Periodontal disease occurs due to chronic inflammation from untreated gingivitis, eventually resulting in gingival connective tissue destruction, alveolar bone resorption and ultimately, tooth loss. Electrospun scaffolds may be used to create tissue engineered constructs to aid in the regeneration of the gingival tissues. However, the use of a synthetic material in the infectious oral environment has the potential to lead to a biomaterial-associated infection [1]. In addition, periodontal pathogens delay or inhibit healing in periodontal tissue regeneration strategies despite systemic and topical administration of antibiotics and antiseptics [2]. Antibiotics incorporated directly into electrospun scaffolds result in antibiotic aggregation, causing changes in the physical properties of the scaffold, and "burst" release of the drug [3]. This latter outcome results only in a short-term introduction of the drug which can potentially result in drug-resistant bacteria growth, future biofilm formation, and ultimately poor healing at and around the implant site [4]. Polymer-based antimicrobial delivery systems have been explored as a means to deliver drugs in a more sustained, controlled manner, which would result in more effective antimicrobial properties [5], [6]. A proprietary antimicrobial polymer containing ciprofloxacin, denoted by "CF (AP)" has been incorporated into aligned electrospun nanofiber scaffolds fabricated using a degradable polycarbonate polyurethane, and the scaffolds' physical properties and drug release characteristics have been characterized. The goal of this thesis project is to evaluate the cell compatibility of the scaffold, in order to assess their suitability as infection resistant tissue engineering scaffolds. In this study, human gingival fibroblasts (HGF) will be used as a representative cell sample as they are the most abundant cell type in the gingival connective tissues, and have a major role in the repair and remodeling of the connective tissue [7].

1.1 Hypothesis

It is hypothesized that biodegradation and antimicrobial release products from the electrospun scaffolds during a 7 day in vitro biodegradation study have no effect on HGF cell numbers and metabolic activity, and that the cells are able to attach on the scaffolds.

1.2 Objectives

The following objectives have been devised to address the above hypothesis:

i. Determine the cytocompatibility of biodegradation and by-products released from electrospun antimicrobial scaffolds. A WST-1 cell metabolic assay and CyQUANT DNA quantification assay will be used to determine any cytotoxic effects of the release products.

ii. Assess HGF attachment on the antimicrobial scaffolds. Scanning electron microscopy (SEM) will be used to determine cell morphology. A live/dead assay in conjunction with confocal microscopy will be used to determine the degree of cellular attachment and cell viability on the scaffold.

Chapter 2

Background

2.1 Periodontal Anatomy and Disease

Periodontal disease occurs due to untreated gingivitis, leading to chronic inflammation of the surrounding tissue. It is characterized by tartar buildup along and into the tooth, and into the periodontal space. This causes an increase in the activity of matrix metalloproteinases (MMPs), enzymes involved in the remodeling of the extracellular matrix (ECM) and basement membrane [9]. Uncontrolled levels of MMPs lead to destruction of the ECM [9]. In teeth, the ECM of interest is the lamina propria, which sup ports the epithelium and constitutes the oral mucosa. Ultimately, this causes alveolar bone resorption and tooth loss due to lowered applied force on the jaw and increased osteoclast activity from inflammation. This disease affects 47% of adults over the age of 30, and is especially prevalent in those over the age of 65, affecting 70% of that age group [10]. Current methods for treating periodontal disease include: scaling and root planning, pocket reduction surgery, gingival or bone grafts, guided tissue regeneration, and dental implants [11], [12].

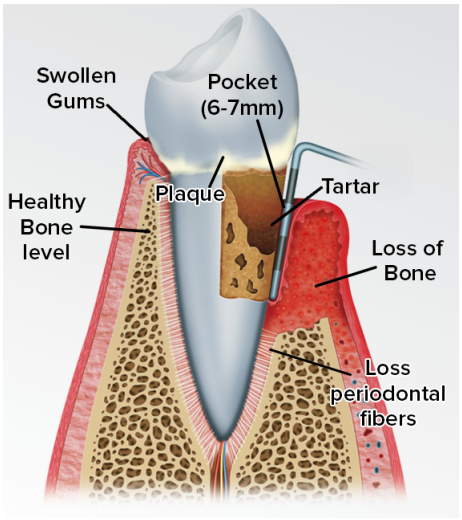

Figure 2.1: Diagram displaying effects of periodontal disease. Adapted from [8].

2.1.1 Oral Mucosa

The periodontium is a complex organ which surrounds and supports the teeth. It consists of several tissue layers: the periodontal ligament (PDL), the cementum, the alveolar bone, and the gingiva [14]. Of importance in this thesis is the gingiva, which acts as a barrier to prevent food or bacterium from entering the deeper periodontal layers. The gingiva primarily consists of an epithelial layer supported by a connective tissue layer, named the lamina propria [15]. The lamina propria is not only responsible for the structure, but also for epithelial nourishment and plays host to some immune cells. It is a highly vascularized tissue, consisting of an extensive network of capillary beds especially near the epithelial layer [15]. Human gingival fibroblasts are one of the most abundant cells in the lamina propria and are responsible for the maintenance of the ECM [15]. This involves secreting ECM components and producing enzymes for ECM remodeling. During wound repair, fibroblasts are responsible for synthesizing ECM matrix proteins such as collagen and fibronectin, growth factors such as vascular endothelial growth factor (VEGF) and transforming growth factor (TGF), as well as remodeling enzymes such as MMPs [9], [15].

2.2 Periodontal Grafts

In the event standard preventative techniques such as scaling and root planning are ineffective, surgical intervention may be required for periodontal disease treatment. In these cases, the gingiva is surgically resected and tarter is removed. The gingiva is then replaced in a way to reduce gaps between it and the tooth to reduce bacterial growth formation. If any supporting tissue has receded or been destroyed, then grafts are required to fix the defect. The current standard of care uses autologous tissue grafts in order to stimulate growth of new cells for tissue regeneration [15]. This method involves using host tissue from the palate. However, the shortcoming with using autologous grafts is that there is a chance of donor site tissue damage or morbidity, tissue shortage, and poor or unpredictable graft healing properties [14], [15]. Gingival tissue engineering may be used to generate full thickness grafts which include all the necessary cells for tissue regeneration ([12], [14], [15]) and address the shortcomings involved

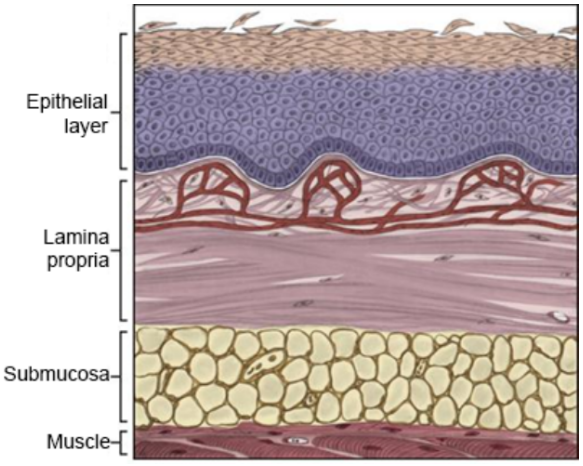

Figure 2.2: Diagram displaying gingival layers. Adapted from [13].

with the use of autologous grafts.

2.2.1 Tissue Engineered Scaffolds from Synthetic Materials

Tissue engineered epithelial sheets are commercially available as an alternative to autologous grafts, but are thin and difficult to use, resulting in poor wound healing [15]. While natural ECM scaffolds can be used, they degrade quickly and are unpredictable, hence why synthetic scaffolds may be a better choice [16], [17]. Synthetic scaffolds can be used to create a full thickness mucosa, which can consist of the necessary cells, nutrients, and growth factors in order to properly regenerate the host tissue. In addition, all aspects of its mechanical and degradation properties can be known in order to predict its behavior *in vivo*. In this thesis, the scaffold platform is an electrospun polycarbonate polyurethane nanofiber. This scaffold has previously been characterized and shown to promote vascular smooth muscle cell attachment [18], and be non-toxic to annulus fibrous cells [19]. Electrospun scaffolds have similar morphological characteristics as native ECM, which will help provide a niche for the cells to grow in [18].

Polyurethanes (PUs) are a class of polymers characterized by urethane links. They were first introduced for cardiovascular applications in the 1960s, and have since been applied to many different biomedical applications due to their physical properties, biocompatibility, and biostability [20]. Biodegradable PUs are designed to undergo hydrolytic or enzymatic degradation of the urethane, urea, ester, ether, or carbonate bonds present in the PU chain. Varying hard and soft segments of the polymer, as well as composition, changes the degradation kinetics and can be used to control the rate of degradation [21]. Specifically, the polyurethane used was a polycarbonate PU synthesized using hexane diisocyanate (HDI), polycarbonate diol (PCN), and butane diol (BD) in a 3:2:1 ratio respectively. When degraded, several small chained products form, including hexane diamine (from the breakdown of HDI), which may be cytotoxic [21].

2.3 Biomaterial Associated Biofilms

Introducing synthetic material in the oral environment has the potential to lead to bacterial biofilm formation, and a host immune response. By controlling both types of interactions, a more predictable material will be created. Bacterial biofilms occur due to adhesion of bacteria on a surface, followed by a thick and tough coating of an extracellular polymeric substance produced by the adhered bacteria [22]. This coating renders immune responses and antibacterial agents less effective, and can increase antibiotic resistance [7], [23], [24]. This results

in a chronic infection and poor wound healing. During this process, immune cells will persist at the site of infection, releasing inflammatory cytokines and enzymes which begin to degrade the surrounding tissue [22]. Any biomaterial used for periodontal tissue engineering will be placed in a highly infective environment due to the nature of the oral cavity. As such, periodontal pathogens delay or inhibit healing in periodontal tissue regeneration strategies involving the use of a implanted biomaterial despite systemic and topical administration of antibiotics and antiseptics [2]. As a result, regenerative approaches using biomaterials may result in failure due to infection [2], [23].

2.4 Polymer-based Drug Delivery and Tissue Engineering

As previously mentioned, bacterial infections can cause complications during the wound healing process. Proper management of the wound post-implant is essential to preventing infection, which can be done by incorporating antibiotics with the material. However, directly incorporating antibiotics into electrospun scaffolds result in antibiotic aggregation, causing changes to the physical properties of the scaffold [3]. In addition, the lack of strong bonds associating the drug with the polymer results in "burst" release of the drug [3]. As such, this outcome results only in a short-term introduction of the drug, only preventing the initial microorganism invasion and growth. In environment such as the oral mucosa, high amounts of microorganisms would mean that this "burst" release can potentially result in drug-resistant bacteria growth, future biofilm formation, and ultimately poor healing at and around the implant site [4]. Thus, a long-term release of the drug is required.

Polymer-based antimicrobial delivery systems have been explored as a means to deliver drugs in a more sustained, controlled manner, which would result in more effective antimicrobial properties [5], [6]. Previous studies have investigated various drug and polymer combinations. Polylactide-co-glycolide (PLGA) has been explored in both disc and electrospun form as methods for long-term drug release [25]–[27]. Another application was to use PLGA as a microparticle drug carrier within a collagen sponge resulting in local drug delivery [28]. Specific to the proposed solution, polyurethanes and fluoroquinolones have also been investigated as a possible polymer-drug combination. There, the drug release profile was proportional to the bacterial infection due to macrophage-mediated enzymatic degradation [5], [6].

2.5 Ciprofloxacin

The antimicrobial used for this application is ciprofloxacin (CF), a second-generation fluoroquinolone. It is a broad-spectrum antibiotic, used to treat many different types of gram negative

and gram positive bacterial pathogens. This type of antibiotic works by selectively inhibiting the topoisomerase II ligase domain, which is responsible for reducing DNA strain during the unwinding process of protein synthesis and mitosis [29]. This results in fragmentation of the DNA, rendering the bacterium unable to produce new proteins required for survival, or divide. It has been shown, however, that ciprofloxacin can also inhibit fibroblast cell proliferation at higher concentrations [29], [30].

2.6 Previous work

Several key elements were done prior to this thesis by Wright et al. [31]. Four scaffolds were created: a 0 wt% AP with no antimicrobial; 7 wt% and 15 wt% CF (AP), where the drug is incorporated in polymer form; and a 15 wt% CF HCl, where the drug is not bound in polymeric form. The 15 wt% CF HCl differs from the 15 wt% CF (AP) in the drug release profile. Since the 15 wt% CF HCl uses free drug, there is a high initial burst drug release of CF at 100x that from scaffolds with CF in polymer form. It serves as a comparison to the 15 wt% CF (AP) in the antimicrobial's ability for a slow release profile. To collect biodegradation and release product samples, sections of scaffold were degraded in phosphate buffered saline (PBS) for 7 days at $37\,^{\circ}\mathrm{C}$. Afterwards, samples were collected and frozen at $-20\,^{\circ}\mathrm{C}$.

Chapter 3

Cytocompatibility studies

3.1 Introduction

The goal of the cytocompatibility studies is to determine any cytotoxic effects of the biodegradation and drug release products from electrospun antimicrobial scaffolds. Initially, the protocol developed by Yeganegi et al. for testing the cytotoxicity of the biodegradation products from electrospun polycarbonate PU was followed [19]. Briefly, cells were seeded onto 96 well plates and incubated for 24 hours. The old culture medium was aspirated, and the biodegradation products were added directly to the wells, or diluted with fresh culture medium as appropriate. However, since the biodegradation products were collected in PBS, the cells were unable to survive for the 24 hour incubation in the test solution, contrary to Yeganegi et al. [19]. This was most likely due to the lack of nutrients and growth factors in the 100% concentrated solution. Further experimentation showed that both Dulbecco's modified Eagle's medium (DMEM) powder and fetal bovine serum (FBS) was required for cell survival, the two main components present in regular culture medium (Figure A.1). The increase in salt concentration from using PBS as a base medium did not show any cytotoxic effects. As a result, a new growth medium (GM) was defined for this set of studies: PBS with DMEM powder and 10% FBS. This ensured that the biodegradation solutions had the necessary nutrients and growth factors for survival, and that any cytotoxic effect was solely due to the release products. To determine if any other aspects of the biodegradation and release products were responsible for the decrease in metabolic activity, two other factors were explored in brief: the accumulation of release products, and solid particulates, using this new GM.

3.2 Materials and Methods

3.2.1 Human gingival fibroblast (HGF) culture

Human gingival fibroblasts (HGF-1, ATCC, CRL-2014) were thawed from $-80\,^{\circ}\mathrm{C}$ cold storage and suspended in DMEM supplemented with 10% FBS (Sigma-Aldrich, St. Louis, MO, USA), and $1\,\mathrm{mM}$ penicillin/streptomycin (Sigma-Aldrich). HGFs were grown to confluence in T75 tissue-treated culture flasks ($37\,^{\circ}\mathrm{C}$, 5% CO_2 cell incubator) and subcultured using standard trypsinization methods. All cell culture techniques were done under aseptic conditions.

3.2.2 Cytocompatibility experiments

24 hours prior to the start of the experiments, HGFs were passaged from a confluent T75 flask and seeded at a density of 10,000 cells/well on sterile tissue-culture treated 96 well plates. The biodegradation products were thawed and supplemented with DMEM powder (Life Technologies, Waltham, MA, USA) at 13.5mg/mL, and 10% FBS (Sigma-Aldrich). These solutions were diluted in equivalent media (GM, DMEM powder and 10% FBS in PBS) to create 90%, 50%, and 10% v/v biodegradation solutions. The old media was removed from each of the wells and the appropriate test solution was added. 10% dimethyl sulfoxide (DMSO, Sigma-Aldrich) in GM was used as the positive control. The cells were incubated for 24 hours ($37\,^{\circ}\mathrm{C}$, 5% CO_2 cell incubator) before assaying. All conditions were run in triplicate and the experiment was repeated 3 times.

3.2.3 Non-soluble Fraction Separation

In this set of experiments, soluble and non-soluble fractions of the biodegradation solution was separated into its soluble and non-soluble components. Soluble and non-soluble fractions were separated by centrifugation at 14,000 RPM for 30 mins. The soluble fraction was transferred to a new tube, and the non-soluble fraction was resuspended in fresh sterile PBS. DMEM powder and FBS were then added.

3.2.4 Cell metabolic activity assay

A WST-1 cell metabolic activity assay was used to measure cell toxicity (Roche Diagnostics, Basel, Switzerland). This assay was performed following manufacturer's instructions. Briefly, 24 hours after the addition of the biodegradation product, the solution in each well was aspirated carefully and replaced with $200\,\mu\mathrm{L}$ of fresh DMEM. $20\,\mu\mathrm{L}$ of WST-1 reagent was added, and the plate was incubated for one hour before reading. The plate was read using a microplate

reader at $450\,\mathrm{nm}$ with a background reading at $690\,\mathrm{nm}$. All readings were subtracted from a well containing growth medium, but no cells. Background readings from wells containing only the biodegradation products were also explored and no difference between growth medium and biodegradation product background wells were found.

3.2.5 CyQUANT DNA quantification assay

The amount of DNA was quantified using a CyQUANT DNA quantification assay (Molecular Probes, Burlington, ON, Canada), and was prepared following manufacturer directions. 24 hours after the addition of the biodegradation product, the solution in each well was aspirated carefully and the plate was frozen at $-80\,^{\circ}\mathrm{C}$ for at least 3 hours to initiate cell lysis. The plate was thawed, and $200\,\mu\mathrm{L}$ of freshly-prepared CyQUANT GR/Lysis buffer reagent was added to each well. The plate was read at a $485\,\mathrm{nm}$ excitation and $530\,\mathrm{nm}$ emission wavelength on a Bio-Tek FL600 Microplate Fluorescence Reader (Bio-Tek, Winooski, VT, USA). The readings were compared to a λ-phage DNA standard.

3.2.6 Statistical Analysis

All statistical analysis were performed using IBM SPSS Statistics 22 (IBM, Somers, NY, USA). A univariate analysis of variance (ANOVA) was performed. Sets with equal variances as determined by Levene's Test with $p < 0.05$ had *post hoc* tests done using Tukey-Kramer HSD, and Dunnett T3 otherwise. All values are presented as mean $\pm$ standard error (SE), and p-values of 0.05 or lower were deemed significant.

3.3 Results

3.3.1 WST metabolic assay

Different concentration gradients of the degradation products were applied to human gingival fibroblasts grown in monolayer culture. WST results are shown in Figure 3.1 with values relative to GM, showing significantly lower activity for the 0 wt% AP ($76.6 \pm 6.0\%$) and 7 wt% CF (AP) ($71.3 \pm 3.7\%$) samples at 90% v/v, and for the 15 wt% CF HCl samples at 90% v/v ($70.7 \pm 7.0\%$) and 50% v/v ($77.9 \pm 5.8\%$). The 15 wt% CF (AP) sample showed a small but statistically insignificant cytotoxic effect at the 90% concentration.

To try and understand the decrease at 90% v/v, the graph can be rearranged to show the effect of antimicrobial polymer concentration at the 90% v/v level, as shown in Figure 3.2. The values for 0 wt% AP ($76.6 \pm 6.0\%$), 7 wt% CF (AP) ($71.3 \pm 3.7\%$), 15 wt% CF (AP)

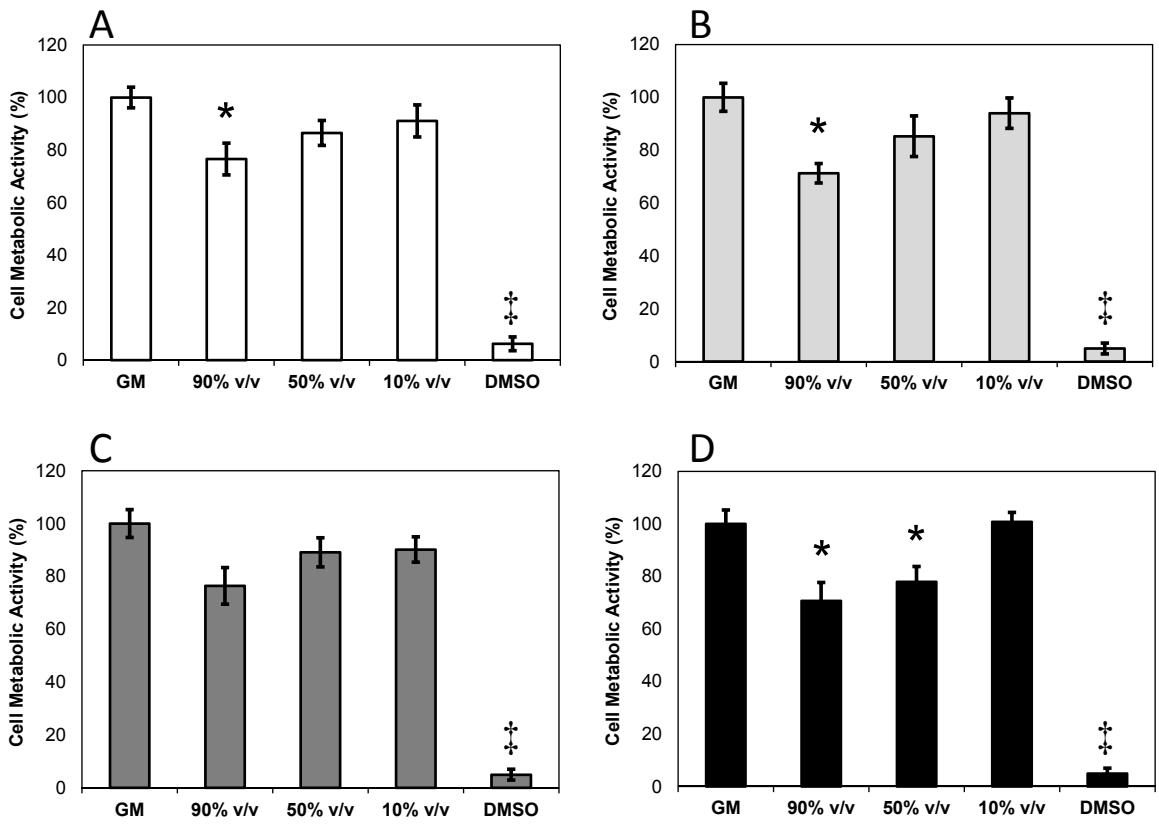

Figure 3.1: Cell metabolic activity relative to GM negative control for all samples. (A) 0 wt% AP, (B) 7 wt% CF (AP), (C) 15 wt% CF (AP), (D) 15 wt% CF HCl. Error bars represent $mean \pm SE$. n = 9. * represents significantly different from GM control, ‡ denotes significantly different from all groups. Decrease in metabolic activity detected in 4 conditions: 90% v/v for 0 wt% AP and 7 wt% CF (AP), and 90% v/v and 50% v/v for 15 wt% CF HCl.

($76.4 \pm 6.9\%$), and 15 wt% CF HCl ($70.7 \pm 7.0\%$) are not significantly different from each other. This means that there is no change in relative metabolic activity across the groups, indicating that the antimicrobial polymer itself is not responsible for the decrease in metabolic activity. It is hypothesized that small molecular weight chains of PU, PU degradation products, residual electrospinning solvent trapped in the scaffold fibres, or even the aged PBS used to create the growth medium for the biodegradation product test solutions may play a role in the lowered metabolic activity.

3.3.2 DNA quantification

DNA quantification results indicate no significant decreases in DNA content from all samples, as seen in Figure 3.3. This indicates that the number of cells, which correlates with the amount

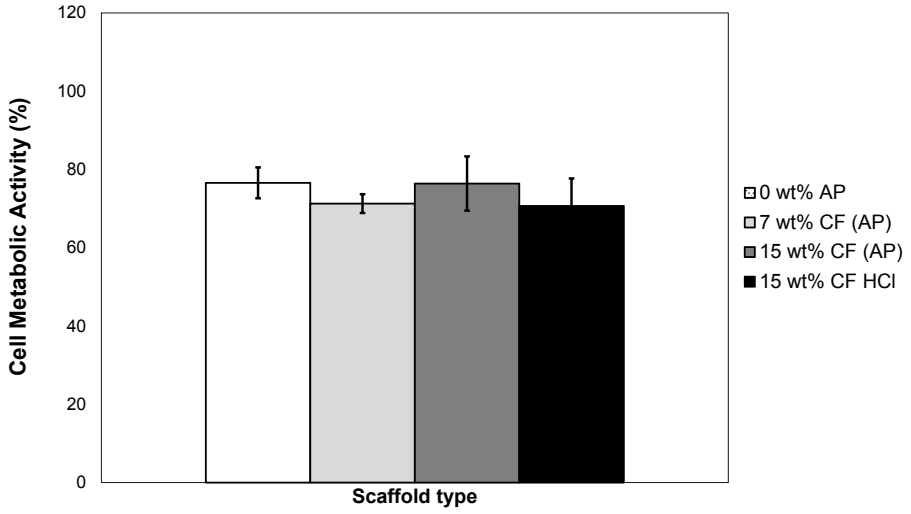

Figure 3.2: Cell metabolic activity results for 90% v/v concentration relative to GM. Error bars represent $mean \pm SE$. n = 9. ‡ denotes significantly different from all groups. No significant difference between each condition.

of DNA, did not change between conditions, meaning that the biodegradation and release products did not reduce cell level relative to the negative control.

3.3.3 Accumulation of release products

The accumulated biodegradation and drug release products from the 0 wt% AP scaffolds after 1 day, 7 days, and 28 days of incubation were examined. Data collected from these experiments in Figure 3.4 showed a decrease in metabolic activity as the amount of release product accumulated. In particular, at 90% v/v concentration, both the 7 day sample ($76.6 \pm 6.0\%$) and the 28 day sample ($61.6 \pm 7.4\%$) showed a decrease in metabolic activity, but no change in DNA levels. In addition, there was also lowered metabolic activity at 50% v/v concentration at day 28 ($61.6 \pm 3.5\%$). This indicated that high concentrations of these release products can play a role in cytotoxic effects. This could be due to high concentrations of both PU degradation products such as HDI, and drug, as previously mentioned in Sections 2.2.1 and 2.5. However, such a high accumulation of release products, especially in the 28 day case, would be physiologically unlikely.

3.3.4 Solid particulates

Yeganegi et al. tested for the cytotoxic effects of the solid particulates in the biodegradation solution [19]. To mirror their experiments, a similar study was conducted. Results indicated

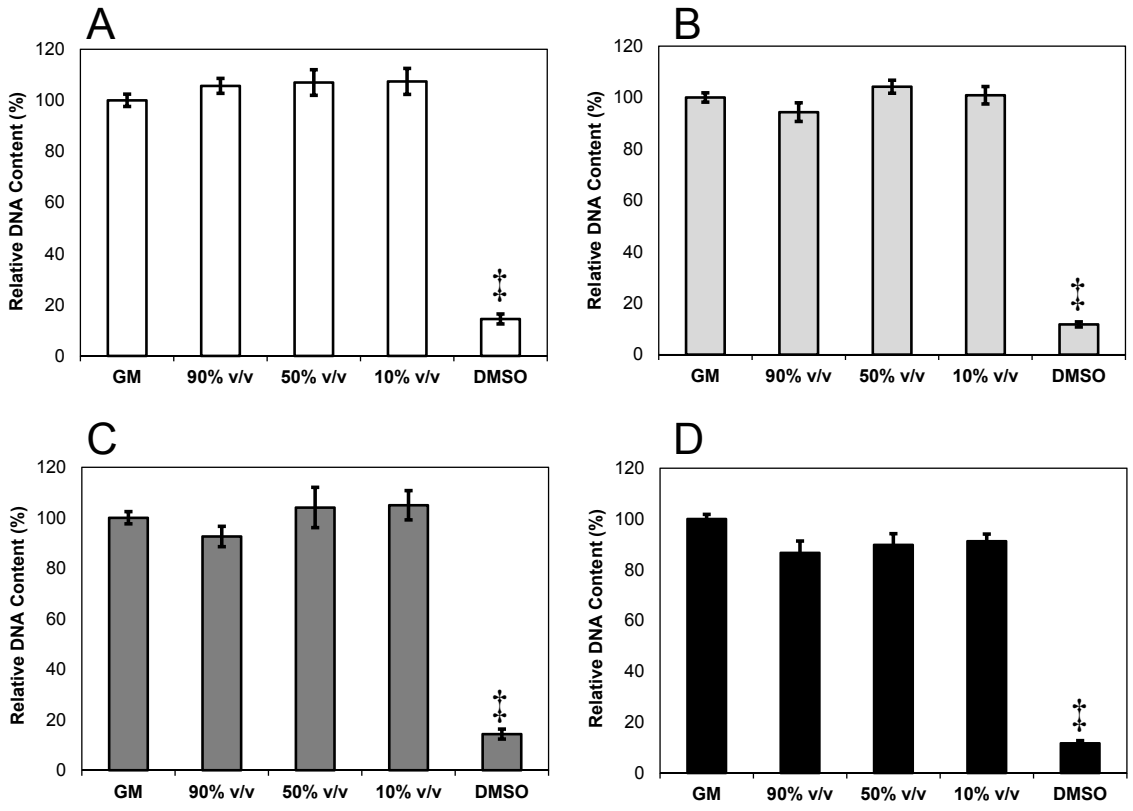

Figure 3.3: DNA content relative to GM negative control. (A) 0 wt% AP, (B) 7 wt% CF (AP), (C) 15 wt% CF (AP), (D) 15 wt% CF HCl. Error bars represent $mean \pm SE$. n = 9. ‡ denotes significantly different from all groups. No significant difference detected for all groups.

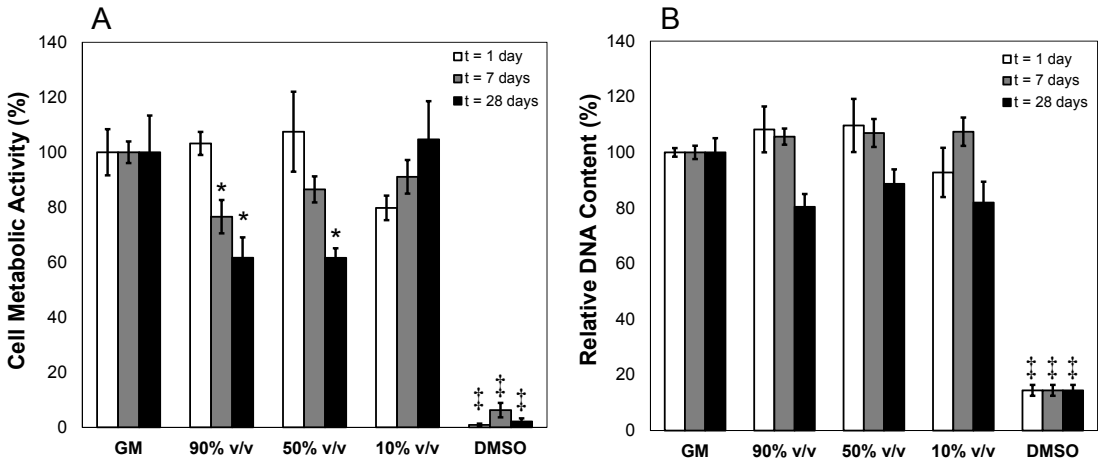

Figure 3.4: Cell metabolic activity and DNA content results looking at cytotoxic effects from the accumulation of release products for the 0 wt% AP samples (A) WST, (B) DNA, relative to GM. Error bars represent $mean \pm SE$. n = 3 (t = 1 day), n = 9 (t = 7 days), n = 6 (t = 28 days). * represents significantly different from GM control, ‡ denotes significantly different from all groups. Cell metabolic activity at 90% v/v drops at 7 days, and at 90% and 50% v/v at 28 days.

that the non-soluble fraction was not responsible for any cytotoxic effects (Figure 3.5). However, there was still a difference between the 90% and 50% v/v concentration and GM for the soluble fraction. From this, it can be concluded that the products responsible for the decrease in metabolic activity can be found in the soluble fraction of the degradation products.

3.4 Discussion

The results indicate a cytotoxic effect of the scaffolds with 0 wt% and 7 wt% drug polymer (reduction in metabolic activity). However, further studies would have to be performed to determine specifically which factors are causing the decrease in metabolic activity.

As previously mentioned, factors such as toxic PU products, residual electrospinning solvent, or aged PBS may have contributed to this effect. It was shown that the 0 and 7 wt% scaffolds showed a greater amount of PU degradation compared to either of the 15 wt% scaffolds [31] and so there should have been a more pronounced difference in the cytotoxicity for the 0 and 7 wt% scaffolds. However, the data does not suggest such a difference. Hexafluoroisopropanol (HFIP) was used as the electrospinning solvent, and is toxic. It is unlikely that HFIP is responsible for the decrease in metabolic activity as the scaffolds were dried prior to biodegradation, meaning that the residual solvent should have evaporated. Furthermore, resid-

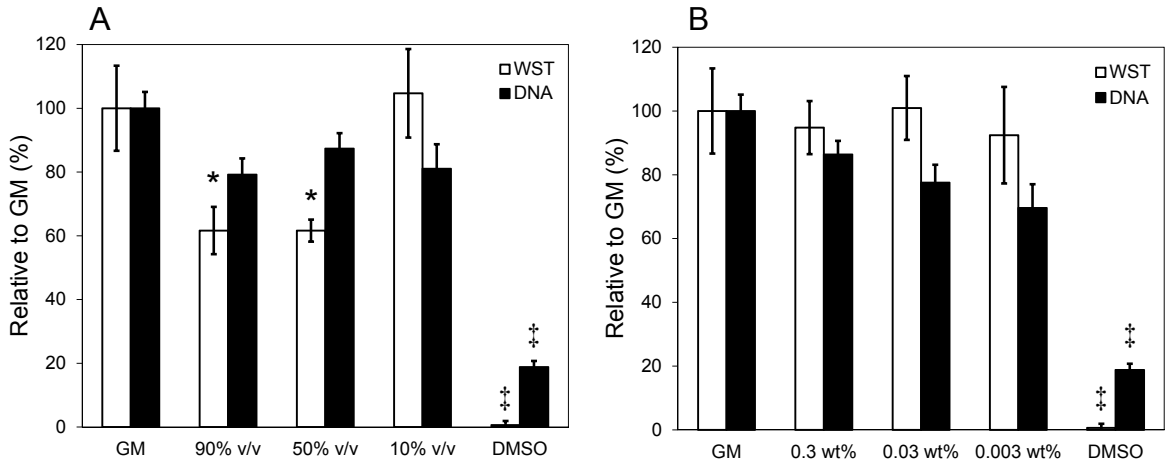

Figure 3.5: Cell metabolic activity and DNA results looking at the cytotoxic effects of (A) soluble and (B) non-soluble release products from 0 wt% AP at t = 28 days. n = 6. * represents significantly different from GM control, ‡ Notice the same trend in the metabolic activity - drops for the 90% and 50% v/v. No significant differences found in DNA.

ual solvent is not expected to continue being released from the scaffolds throughout the 28 day study, yet there is a greater effect on cell metabolic activity for the 28 day release products than the 7 day release products. Residual solvent would most likely come off the scaffolds in the first few days of incubation, and there is no cytotoxic effect for the 1 day release products. The last possible factor would be the aged PBS. The potential cytotoxic effect of aged PBS is currently being investigated.

Interestingly, the 15 wt% CF (AP) sample showed no cytotoxic effect at any concentration, despite the 15 wt% CF HCl sample showing cytotoxic effect at both 90% and 50% v/v. This suggests that there is some protective mechanism provided by the antimicrobial polymer. That is, when the drug is bound in the polymeric form, it may not interact with the cells in the same manner as free drug. However, this may also affect the ability for the drug to interact with bacterium for its antimicrobial property. WST is reported to measure cytotoxicity, but more specifically is an indicator of cell metabolic activity. There are other factors which could lead to lower metabolic activity, but not necessarily decrease cell viability, including a confluent culture and senescence [32]. Metabolic activity would be lower in these cases compared to actively dividing cells. As such, DNA quantification was used to support the data from the WST assay. However, DNA quantification indicated no change, meaning that the lower cell metabolic activity was not caused by a smaller cell population and that some factor, other than cell death and detachment, was responsible for the lowered metabolic activity.

Physiologically, it is not expected that such a high concentration of release product would be present. Constant exchanges of fluid, especially in such a vascularized tissue, would remove these products before such high accumulation would occur. This means that the results here may not be directly representative of that in an *in vivo* system, but more closely follow the 1 day time point result. This work has concentrated on investigating possible effects of the biodegradation and release products on cell viability. Future studies are required to explore other measures of cell function, such as cell proliferation and ECM synthesis.

Chapter 4

Cell seeding studies

4.1 Introduction

The goal of the cell seeding studies was to determine if HGF cells are able to attach to the scaffolds. Initially, the apparatus developed by Turner et al. was adapted for this specific scaffold and cell type [33]. However, gamma sterilization of these scaffolds lead them to become brittle, creating holes within the membrane and preventing cell attachment. As such, a new scaffold holder was purchased, the CellCrown 96 from Scaffdex Ltd. This allowed for the scaffolds to be secured, and created a well for the culture medium. However, it was not sufficient for adequate cell adhesion. Yang et al. showed that an increase in the material surface polar character and the presence of surface proteins aided cell attachment [34]. As such, pre-wetting would help increase the surface polar characteristic, and the addition of serum-media would allow for the pre-adsorption of proteins. However, given the initial burst drug release of the antimicrobial scaffolds, the cell seeding protocol needed to be optimized to prevent high drug loss. As such, only enough culture medium was used to pre-wet the cell to ensure that any effects on cell attachment from the loaded drug remained.

4.2 Materials and Methods

4.2.1 Human gingival fibroblast (HGF) culture

Human gingival fibroblasts were thawed from $-80\,^{\circ}\mathrm{C}$ cold storage and suspended in DMEM supplemented with 10% FBS, and $1\,\mathrm{mM}$ penicillin/streptomycin. HGFs were grown to confluence in T75 tissue-treated culture flasks ($37\,^{\circ}\mathrm{C}$, 5% CO_2 cell incubator) and subcultured using standard trypsinization methods. All cell culture techniques were done under aseptic conditions.

4.2.2 Cell seeding

Scaffolds were secured onto CellCrown 96 (Scaffdex Ltd., Tampere, Finland) scaffold holders and placed in wells of a 96 well plate. $15\,\mu L$ of media was added to wet the surface of the scaffold, which was then incubated at $37\,^{\circ}C$, 5% CO_2, for 1 hour prior to seeding. HGFs were passaged from a confluent T75 flask, and seeded at a density of 5,000 cells/scaffold in $25\,\mu L$ of media. Cells were incubated for another hour at the same conditions to allow for cell attachment. Afterwards, an additional $125\,\mu L$ of media was added, and the plate was returned to the incubator. The cells were incubated for 24 hours before assaying.

4.2.3 Scanning electron microscopy

Scanning electron microscopy (SEM) was used to determine the morphology of the cells on the scaffold post-seeding. In preparation for SEM, the scaffolds were washed 3 times with PBS and fixed using 3% gluteraldehyde (Sigma-Aldrich). They were then dehydrated in increasing amounts of ethanol (30%, 50%, 70%, and 90%) for an hour each before switching to 95% ethanol overnight. The following morning, the samples were switched to 100% ethanol for an hour before critical point drying. Then the samples were mounted to steel studs using carbon tape and sputter-coated with platinum using an SC515 SEC Coating unit. Samples were then imaged using a Hitachi S2500 SEM (Hitachi, Mito City, Japan).

4.2.4 Live/Dead cell viability assay

Live/Dead reagent (Molecular Probes, Burlington, ON, Canada) was used to determine cell viability and prepared according to manufacturer instructions. In preparation for the assay, the culture plate was removed from the incubator and the media aspirated. Scaffolds were washed 3 times in PBS(+/+) (PBS with $MgCl_2$ and $CaCl_2$) for 5 minutes on a plate shaker. $100\,\mu L$ of the live/dead reagent was added to the surface and incubated for 30 minutes at room temperature in the dark. After incubation, the scaffolds were washed again with PBS(+/+) for 5 minutes on the plate shaker, 3 times. On the final wash, $150\,\mu L$ of PBS at pH 7.4 was added to each well before imaging. Samples are then viewed using a Zeiss LSM700 confocal microscope (Carl Zeiss AG, Oberkochen, Germany) with filters of 485/530 nm for calcein, and 530/645 nm for ethidium homodimer-1 (EthD-1) at the Advanced Optics Microscopy Facility (MaRS Center, Toronto, ON, Canada). In this assay, Calcein AM is enzymatically converted to its fluorescent variant, which for viable cells, is concentrated within the cytoplasm. EthD-1 enters the membrane of damaged cells, and binds with nucleic acids where it becomes fluorescent.

4.3 Results

4.3.1 SEM Imaging

SEM indicated that cells were able to attach to the surface of the scaffold (Figure 4.1). Note that cell coverage is not very high, which may be attributed to the previously mentioned issues with pre-wetting, which play a large role in ensuring good cell adhesion [34]. Furthermore, issues with sample preparation resulted in images which were not necessarily representative of typical fibroblast morphology, including cracked edges, wrinkling, and a more square-shaped morphology instead of elongated [35], [36].

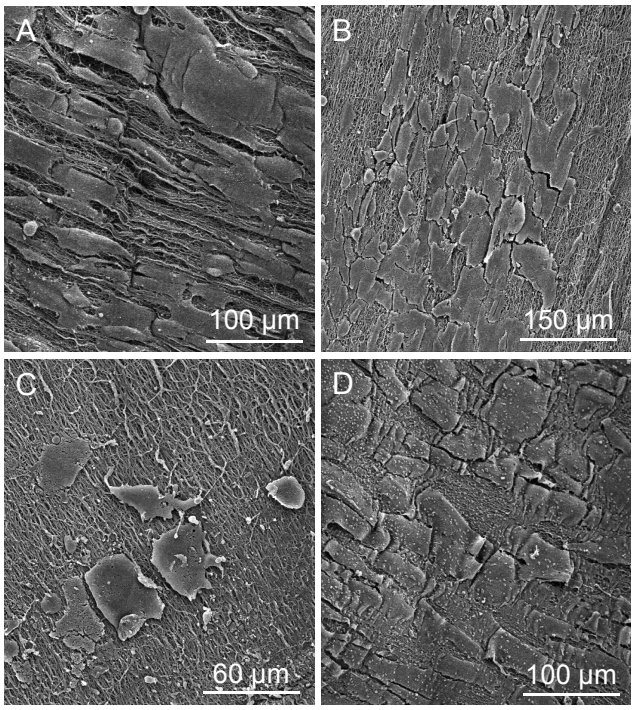

Figure 4.1: Representative SEM images of the scaffolds. (A) 0 wt% AP, (B) 7 wt% CF (AP), (C) 15 wt% CF (AP), (D) 15 wt% CF HCl.

4.3.2 Live/Dead Imaging

Live/Dead confocal imaging indicated that the cells were not only able to adhere to the scaffold, but also were viable. Most notably, cells were fluorescing green, indicating cell viability, and only very few cells were fluorescing red, indicating cell death (Figure 4.2). Cell morphology indicates that the HGF cells are spread out with a morphology appearing similar to that of typical fibroblasts. Results for this experiment were inconsistent as not all scaffolds imaged

resulted in cell attachment. As such, it cannot be concluded as to if antimicrobial concentration plays a role in cell adhesion.

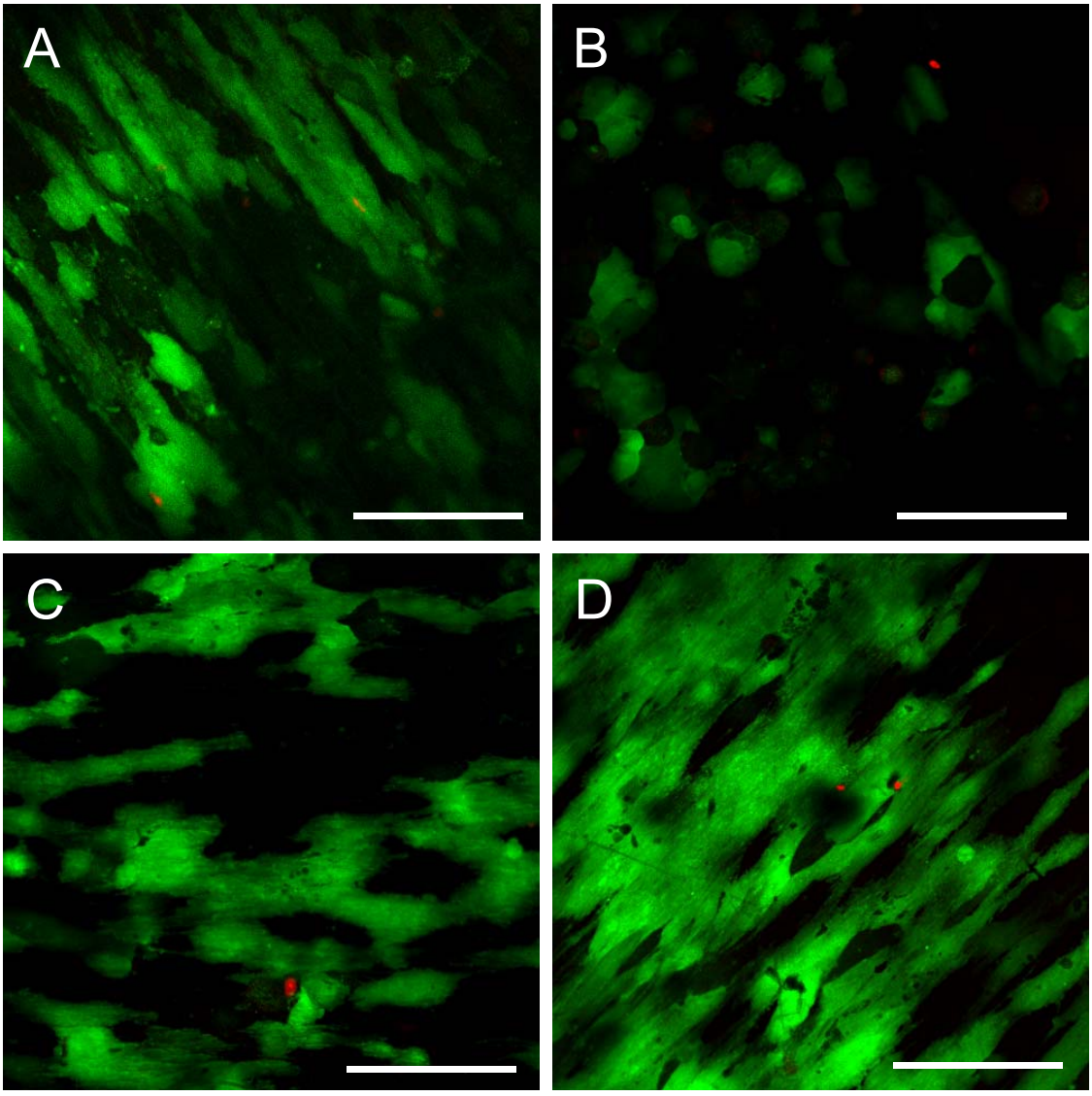

Figure 4.2: Representative live/dead confocal images of HGF cells seeded on scaffolds after 24 hours. (A) 0 wt% AP, (B) 7 wt% CF (AP), (C) 15 wt% CF (AP), (D) 15 wt% CF HCl. Green represents live cells (Calcein), whereas red represents dead cells (EthD-1). All scale bars represent $200\,\mu\mathrm{m}$. Results indicate that cells are viable.

4.4 Discussion

The goal of using electrospun scaffolds was to create a physical environment which mimics the natural ECM, thus enhancing cell attachment [18]. From the SEM and confocal live/dead stain images, it can be concluded that cells are able to adhere to the scaffold and remain viable, confirming our hypothesis. However, poor cell seeding efficiency and inconsistent results limits the ability to perform a detailed analysis of cell viability or morphology.

One aspect of the wetting process which promotes cell attachment is serum, which contains high levels of proteins, and other factors. Pre-wetting with serum allows for protein adsorption on the surface, and more specifically, adhesion proteins such as vitronectin and fibronectin [37]. This would allow for high cell adhesion on surfaces without high hydrophilic regions or polar character [34], [37]. Previous results indicated that each of the scaffolds had a different hydrophobic characteristic [31]. The 0 wt% AP scaffold had the highest contact angle, or was the most hydrophobic, followed by the 7 wt% CF (AP), and then the 15 wt% CF (AP) and CF HCl. In trials in which the scaffold were not pre-wetted showed little cell attachment on the 0 wt% AP scaffolds and some cell attachment to the 15 wt% CF HCl scaffolds, indicating that hydrophobicity does play a role in this type of scaffold (data not shown). However, in the images presented where the scaffolds have been pre-wetted, it can be seen that the attachment appears to be better in all cases. This reinforces the fact that both surface chemistry and the presence of serum plays a role in enhancing cell attachment.

Chapter 5

Future Work

5.1 Cell attachment studies

Future work of the cell attachment studies would be to further refine the protocol to enhance seeding reliability and efficacy. From there, additional studies could be performed to quantify cell viability on the scaffolds. Additional work also needs to be performed to examine cell morphology via SEM.

5.2 Bacterial inhibition

The goal of this project was to evaluate the scaffolds' cell compatibility to be used as infection resistant scaffolds. One other aspect which was not discussed in this thesis is the ability for the biodegradation and release products to inhibit bacterial growth. Future work would include the release product's toxicity to typical oral bacterium such as *Porphyromonas gingivalis* by calculating the minimum inhibitory concentration, and a zone of inhibition assay on the scaffold itself. These two assays would give a good understand of the antimicrobial efficacy of the scaffolds.

5.3 *In vivo* models

Next steps after looking at bacterial inhibition would be to test these scaffolds *in vivo*. *in vitro* studies, such as the ones performed, are not always indicative of *in vivo* performance. This would involve using animal models to determine if this scaffold is able to allow for gingival repair and prevent bacterial colony formation.

Chapter 6

Conclusion

Periodontal disease occurs due to chronic inflammation from untreated gingivitis, ultimately leading to tooth loss. Electrospun scaffolds may be used to create tissue engineered constructs to aid in the regeneration of the gingival tissues. An electrospun scaffold with an embedded proprietary antimicrobial polymer has been created to address this gap, and this thesis aims to characterize its cell compatibility properties. Results indicate that for 7 day release products, there is decreased cell metabolic activity at the highest concentration due to. However, this decrease in metabolic activity may not occur *in vivo* due to constant circulation of fluids around the body that would remove any biodegradation products affecting cell fate. In addition, HGF cells are able to attach to the scaffold and remain viable after a 24 hour incubation. As such, this electrospun scaffold has promise to be an infection resistant tissue engineering scaffolds for use in the gingiva.

References

[1] J. M. Anderson, "Inflammation, wound healing, and the foreign-body response," in *Biomaterials Science: An Introduction to Materials in Medicine*, B. D. Ratner, A. S. Hoffman, F. J. Schoen, and J. E. Lemons, Eds., 3rd, Elsevier, 2013, ch. II.2.2, pp. 503–512, ISBN: 0-12-582461-0. DOI: 10.1016/B978-0-08-087780-8.00027-9.

[2] M. C. Bottino, V. Thomas, G. Schmidt, Y. K. Vohra, T. M. G. Chu, M. J. Kowolik, and G. M. Janowski, "Recent advances in the development of gtr/gbr membranes for periodontal regeneration - a materials perspective," *Dental Materials*, vol. 28, pp. 703–721, 2012, ISSN: 01095641. DOI: 10.1016/j.dental.2012.04.022.

[3] A. Toncheva, D. Paneva, V. Maximova, N. Manolova, and I. Rashkov, "Antibacterial fluoroquinolone antibiotic-containing fibrous materials from poly(l-lactide-co-d,l-lactide) prepared by electrospinning," *European Journal of Pharmaceutical Sciences*, vol. 47, pp. 642–651, 2012, ISSN: 09280987. DOI: 10.1016/j.ejps.2012.08.006.

[4] A. L. Dumitrescu, *Etiology and Pathogenesis of Periodontal Disease*. Berlin: Springer-Verlag, 2010.

[5] M. Yang and J. P. Santerre, "Utilization of quinolone drugs as monomers: characterization of the synthesis reaction products for poly(norfloxaxin diisocyanatododecane polycaprolactone)," *Biomacromolecules*, vol. 2, pp. 134–141, 2001, ISSN: 15257797. DOI: 10.1021/bm000087g.

[6] G. L. Woo, M. W. Mittelman, and J. P. Santerre, "Synthesis and characterization of a novel biodegradable antimicrobial polymer.," *Biomaterials*, vol. 21, no. 12, pp. 1235–46, Jun. 2000, ISSN: 0142-9612. DOI: 10.1016/S0142-9612(00)00003-X.

[7] J. Taba, Q. Jin, J. V. Sugai, and W. V. Giannobile, "Current concepts in periodontal bioengineering," *Orthodontics and Craniofacial Research*, vol. 8, pp. 292–302, 2005, ISSN: 16016335. DOI: 10.1111/j.1601-6343.2005.00352.x.

[8] Monash Dental Group, *Dental education for patients*, Clayton, Australia, 2015. [Online]. Available: http://monashdentalgroup.com.au/dental-education/.

[9] E. Andrian, Y. Mostefaoui, M. Rouabhia, and D. Grenier, "Regulation of matrix metalloproteinases and tissue inhibitors of matrix metalloproteinases by porphyromonas gingivalis in an engineered human oral mucosa model," *Journal of Cellular Physiology*, vol. 211, no. 1, pp. 56–62, 2006. DOI: 10.1002/JCP.

[10] P. I. Eke, B. a. Dye, L. Wei, G. O. Thornton-Evans, and R. J. Genco, "Prevalence of periodontitis in adults in the united states: 2009 and 2010.," *Journal of Dental Research*, vol. 91, no. 10, pp. 914–20, Oct. 2012, ISSN: 1544-0591. DOI: 10.1177/0022034512457373.

[11] P. Axelsson and J. Lindhe, "The significance of maintenance care in the treatment of periodontal disease," *Journal of Clinical Periodontology*, no. 1971, pp. 281–294, 1981.

[12] C. Dahlin, A. Linde, J. Gottlow, and S. Nyman, "Healing of bone defects by guided tissue regeneration.," *Plastic and reconstructive surgery*, vol. 81, no. 5, pp. 672–676, 1988, ISSN: 0032-1052.

[13] Pocket Dentistry, *9 - oral mucosa*, 2015. [Online]. Available: http://pocketdentistry.com/9-oral-mucosa/.

[14] B. B. Benatti, K. G. Silvério, M. Z. Casati, E. A. Sallum, and F. H. Nociti, "Physiological features of periodontal regeneration and approaches for periodontal tissue engineering utilizing periodontal ligament cells.," *Journal of bioscience and bioengineering*, vol. 103, no. 1, pp. 1–6, Jan. 2007, ISSN: 1389-1723. DOI: 10.1263/jbb.103.1.

[15] K. Moharamzadeh, I. M. Brook, R. Van Noort, A. M. Scutt, and M. H. Thornhill, "Tissue-engineered oral mucosa: a review of the scientific literature.," *Journal of dental research*, vol. 86, no. 2, pp. 115–24, Feb. 2007, ISSN: 0022-0345.

[16] L. Ma, C. Gao, Z. Mao, J. Zhou, J. Shen, X. Hu, and C. Han, "Collagen/chitosan porous scaffolds with improved biostability for skin tissue engineering," *Biomaterials*, vol. 24, no. 26, pp. 4833–4841, 2003, ISSN: 01429612. DOI: 10.1016/S0142-9612(03)00374-0.

[17] Q. Ye, G. Zünd, P. Benedikt, S. Jockenhoevel, S. P. Hoerstrup, S. Sakyama, J. a. Hubbell, and M. Turina, "Fibrin gel as a three dimensional matrix in cardiovascular tissue engineering," *European Journal of Cardio-thoracic Surgery*, vol. 17, no. 5, pp. 587–591, 2000, ISSN: 10107940. DOI: 10.1016/S1010-7940(00)00373-0.

[18] P. H. Blit, K. G. Battiston, M. Yang, J. Paul Santerre, and K. A. Woodhouse, "Electrospun elastin-like polypeptide enriched polyurethanes and their interactions with vascular smooth muscle cells," *Acta Biomaterialia*, vol. 8, pp. 2493–2503, 2012, ISSN: 17427061. DOI: 10.1016/j.actbio.2012.03.032.

[19] M. Yeganegi, R. A. Kandel, and J. P. Santerre, "Acta biomaterialia characterization of a biodegradable electrospun polyurethane nanofiber scaffold : mechanical properties and cytotoxicity," *Acta Biomaterialia*, vol. 6, no. 10, pp. 3847–3855, 2010, ISSN: 1742-7061. DOI: 10.1016/j.actbio.2010.05.003.

[20] S. Guelcher, "Biodegradable polyurethanes: synthesis and applications in regenerative medicine.," *Tissue engineering. Part B, Reviews*, vol. 14, no. 1, pp. 3–17, 2008, ISSN: 1937-3368. DOI: 10.1089/teb.2007.0133.

[21] Y. W. Tang, R. S. Labow, and J. P. Santerre, "Enzyme-induced biodegradation of polycarbonate polyurethanes: dependence on hard-segment concentration," *Journal of Biomedical Materials Research*, vol. 56, no. 4, pp. 516–528, 2001, ISSN: 00219304. DOI: 10.1002/1097-4636(20010915)56:4<516::AID-JBM1123>3.0.CO;2-B.

[22] P. Stoodley, L. Hall-Stoodley, B. Costerton, P. DeMeo, M. Shirtliff, E. Gawalt, and S. Kathji, "Biofilms, biomaterials, and device-related infections," in *Biomaterials Science: An Introduction to Materials in Medicine*, B. D. Ratner, A. S. Hoffman, F. J. Schoen, and J. E. Lemons, Eds., 3rd, Elsevier, 2013, ch. II.2.8, pp. 565–583.

[23] J. Slots, E. S. MacDonald, and H. Nowzari, "Infectious aspects of periodontal regeneration.," *Periodontology 2000*, vol. 19, no. 1, pp. 164–72, Feb. 1999, ISSN: 0906-6713. DOI: 10.1111/j.1600-0757.1999.tb00154.x.

[24] A. Buret, K. H. Ward, M. E. Olson, and J. W. Costerton, "An in vivo model to study the pathobiology of infectious biofilms on biomaterial surfaces.," *Journal of biomedical materials research*, vol. 25, no. 7, pp. 865–74, Jul. 1991, ISSN: 0021-9304. DOI: 10.1002/jbm.820250706.

[25] J. Y. Yoo, J. M. Kim, G. Khang, M. S. Kim, S. H. Cho, H. B. Lee, and Y. S. Kim, "Effect of lactide/glycolide monomers on release behaviors of gentamicin sulfate-loaded plga discs," *International Journal of Pharmaceutics*, vol. 276, no. 1-2, pp. 1–9, 2004, ISSN: 03785173. DOI: 10.1016/j.ijpharm.2004.01.043.

[26] K. Kim, Y. K. Luu, C. Chang, D. Fang, B. S. Hsiao, B. Chu, and M. Hadjiargyrou, "Incorporation and controlled release of a hydrophilic antibiotic using poly(lactide-co-glycolide)-based electrospun nanofibrous scaffolds," *Journal of Controlled Release*, vol. 98, no. 1, pp. 47–56, 2004, ISSN: 01683659. DOI: 10.1016/j.jconrel.2004.04.009.

[27] Y. K. Luu, K. Kim, B. S. Hsiao, B. Chu, and M. Hadjiargyrou, "Development of a nanostructured dna delivery scaffold via electrospinning of plga and pla-peg block copolymers," *Journal of Controlled Release*, vol. 89, no. 2, pp. 341–353, 2003, ISSN: 01683659. DOI: 10.1016/S0168-3659(03)00097-X.

[28] S. H. Lee, J. E. Lee, W. Y. Baek, and J. O. Lim, "Regional delivery of vancomycin using pluronic f-127 to inhibit methicillin resistant staphylococcus aureus (mrsa) growth in chronic otitis media in vitro and in vivo," *Journal of Controlled Release*, vol. 96, no. 1, pp. 1–7, 2004, ISSN: 01683659. DOI: 10.1016/j.jconrel.2003.12.029.

[29] A. Gürbay, C. Garrel, M. Osman, M. J. Richard, A. Favier, and F. Hincal, "Cytotoxicity in ciprofloxacin-treated human fibroblast cells and protection by vitamin e.," *Human & experimental toxicology*, vol. 21, no. 12, pp. 635–641, 2002, ISSN: 09603271. DOI: 10.1191/0960327102ht305oa.

[30] R. J. Williams, E. Attia, T. L. Wickiewicz, and J. a. Hannafin, "The effect of ciprofloxacin on tendon, paratenon, and capsular fibroblast metabolism.," *The American journal of sports medicine*, vol. 28, no. 3, pp. 364–369, 2000, ISSN: 0363-5465. DOI: 10.1097/BLO.0b013e3180e79c6a.

[31] M. Wright and J. P. Santerre, "Anti-infective tissue engineered gingival constructs using multiplatform polyurethane scaffolds and perfused co-culture," Unpublished, Unpublished, 2015.

[32] J. W. Cheung, D. Jain, C. McCulloch, and P. Santerre, "Pro-angiogenic character of endothelial cells and gingival fibroblasts co-cultures in perfused degradable polyurethane (d-phi) scaffolds," *Tissue Engineering Part A*, vol. 21, p. 150 128 190 645 003, 2015, ISSN: 1937-3341. DOI: 10.1089/ten.TEA.2014.0548.

[33] K. G. Turner, N. Ahmed, J. P. Santerre, and R. A. Kandel, "Modulation of annulus fibrosus cell alignment and function on oriented nanofibrous polyurethane scaffolds under tension," *The Spine Journal*, vol. 14, no. 3, pp. 424–434, 2014, ISSN: 1529-9430. DOI: 10.1016/j.spinee.2013.08.047.

[34] L. Yang, R. a. Kandel, G. Chang, and J. P. Santerre, "Polar surface chemistry of nanofibrous polyurethane scaffold affects annulus fibrosus cell attachment and early matrix accumulation," *Journal of Biomedical Materials Research - Part A*, vol. 91, no. 4, pp. 1089–1099, 2009, ISSN: 15493296. DOI: 10.1002/jbm.a.32331.

[35] M. Chen, P. K. Patra, S. B. Warner, and S. Bhowmick, "Role of fiber diameter in adhesion and proliferation of nih 3t3 fibroblast on electrospun polycaprolactone scaffolds.," *Tissue engineering*, vol. 13, no. 3, pp. 579–587, 2007, ISSN: 1076-3279. DOI: 10.1089/ten.2007.13.ft-340.

[36] J. Meng, H. Kong, Z. Han, C. Wang, G. Zhu, S. Xie, and H. Xu, "Enhancement of nanofibrous scaffold of multiwalled carbon nanotubes/polyurethane composite to the fibroblasts growth and biosynthesis," *Journal of Biomedical Materials Research - Part A*, vol. 88, no. 1, pp. 105–116, 2009, ISSN: 15493296. DOI: 10.1002/jbm.a.31862.

[37] E. G. Hayman, M. D. Pierschbacher, S. Suzuki, and E. Ruoslahti, "Vitronectin–a major cell attachment-promoting protein in fetal bovine serum.," *Experimental cell research*, vol. 160, no. 2, pp. 245–258, 1985, ISSN: 00144827. DOI: 10.1016/0014-4827(85)90173-9.

Appendix A

A.1 Growth media formulation

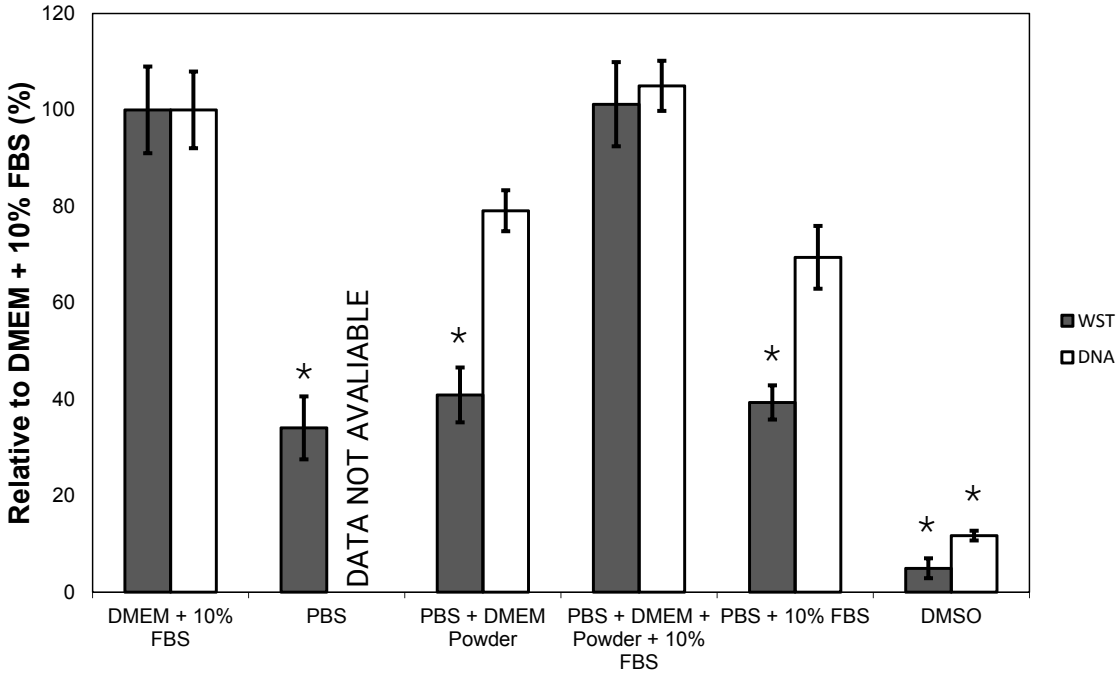

Figure A.1: Relative metabolic activity and DNA content of HGF cells incubated with various culture medium mixtures relative to typical growth medium (DMEM + 10% FBS). Error bars represent $mean \pm SE$. n = 3. * represents significantly different from GM control, ‡ denotes significantly different from all groups. This experiment was performed to determine which other factors were needed to ensure cell viability since PBS alone in the degradation solutions had a strong cytotoxic effect on the cells. The results indicate that both DMEM powder and 10% FBS added to PBS was required to prevent cytotoxic effects due to the culture medium alone.